Tribological properties and wear prediction model of TiC particles reinforced Ni-base alloy composite coatings

Ye-fa TAN, Long HE, Xiao-long WANG, Xiang HONG, Wei-gang WANG

College of Field Engineering, PLA University of Science and Technology, Nanjing 210007, China

Abstract: TiC particles reinforced Ni-based alloy composite coatings were prepared on 7005 aluminum alloy by plasma spray. The effects of load, speed and temperature on the tribological behavior and mechanisms of the composite coatings under dry friction were researched. The wear prediction model of the composite coatings was established based on the least square support vector machine (LS-SVM). The results show that the composite coatings exhibit smaller friction coefficients and wear losses than the Ni-based alloy coatings under different friction conditions. The predicting time of the LS-SVM model is only 12.93% of that of the BP-ANN model, and the predicting accuracies on friction coefficients and wear losses of the former are increased by 58.74% and 41.87% compared with the latter. The LS-SVM model can effectively predict the tribological behavior of the TiC_P/Ni-base alloy composite coatings under dry friction.

Key words: TiC particles; Ni-based alloy; composite coating; least square support vector machine (LS-SVM); wear prediction model

1 Introduction

Aluminum alloys have been used in a wide range of areas, such as aerospace industry, petrochemical industry and weapon industry due to their low density, high specific strength and excellent electrical and thermal conductivity [1−4]. However, the low hardness and poor wear resistance restrain their applications under frictional working conditions. As is known, Ni-based alloys possess good anti-wear, anti-corrosion and anti-oxidation properties, which are widely used as strengthening coatings to enhance the wear resistance of metals [5−8]. To meet the needs of increasingly severe friction conditions, including heavy load, high speed and high temperature, Ni-based alloys coatings reinforced by TiC particles may be a hopeful way to improve the tribological properties and prolong the service life [9,10].

Service life of aluminum alloy friction parts largely depends on wear conditions of strengthening coatings. Indeed, friction coefficient and wear loss are the key indices to evaluate wear conditions, but are notably affected by exterior factors, such as load, speed, temperature, lubrication and humidity. Moreover, there exist typical nonlinear relationships among these factors making it hard to predict the tribological behavior by numerical calculation. Therefore, the accurate prediction on friction coefficient and wear loss of the strengthening coatings under different friction conditions counts for much in grasping their wear conditions and instructing their applications.

Least square support vector machine (LS-SVM) is a pattern recognition and regression analysis structure based on statistics theory and structure risk minimum criterion [11,12]. It integrates square error variable into traditional SVM that substitutes least square linear system for quadratic programming to resolve function estimating problems, which shows good generalization performance and calculation speed in dealing with multivariate nonlinear problems by small samples [13,14]. Recently, some researches on the wear prediction of materials by LS-SVM were carried out. LU et al [15] found that the LS-SVM model showed better predictive speed and accuracy in the wear prediction of bearing steel than the neural network model. WAN [16] created a wear prediction model of centrifugal pump by LS-SVM and SHI et al [17] established a LS-SVM prediction model on lifetime of hard alloy tools. Both models exhibited relatively consistent prediction results with the experiment values. Obviously, excellent prediction effects on tribological behaviors by LS-SVM are obtained. Current researches mostly focus on simple

materials, but little attention is paid to the composite coatings that were extensively used in engineering fields.

In this work, TiC particles reinforced Ni-based alloy (TiC$_P$/Ni-based alloy) composite coatings were prepared on the surface of 7005 aluminum alloy by plasma spray. The tribological properties of the composite coatings at different loads, speeds and temperatures under dry friction condition were investigated. The LS-SVM prediction model on tribological behavior of the composite coatings was created and its predictive effects were compared with the back propagation artificial neural network (BP-ANN) prediction model. The aim of the present work is to provide an effective method for wear condition prediction and service life evaluation of strengthening coatings on aluminum alloys as friction parts under dry friction conditions.

2 Experimental

2.1 Specimen preparation

Spraying materials were composed of Ni-based alloy powder and TiC particles with a volume ratio of 4:1. The chemical composition of the Ni-based alloy powder with the size of 55−128 μm was 15.5% Cr, 3.5% B, 4.0% Si, 15.0% Fe, 3.0% W, 0.8% C and 58.2% Ni (mass fraction), respectively. The TiC particles with size in the range of 4−6 μm were used as reinforcing particles.

7005 aluminum alloy was selected as substrates, which was treated by sanding, ultrasonic degreasing and sandblasting before spraying. The TiC$_P$/Ni-based alloy composite coatings were deposited on the surface of the substrate by a DH−1080 plasma spray equipment. The technical parameters were electric current of 500 A, voltage of 60 V, argon flux of 60 L/min, hydrogen flux of 10 L/min and spray distance of 100 mm. The sprayed specimens were ground by diamond wheel and diamond grease to the surface roughness of 0.5 μm, and then were incised into test pieces with dimensions of 12 mm× 12 mm×6 mm by wire-electrode cutting.

2.2 Testing methods

Tribological tests were carried out on an HT−500 ball-on-disc tribometer. The upper specimen was a GCr15 steel ball and the lower specimen was the sprayed test piece. The GCr15 steel ball slid against the coating under dry friction condition for a distance of 300 m at air humidity of 80%. The test conditions were loads of 3, 6, 9 and 12 N, speeds of 0.14, 0.28, 0.42 and 0.56 m/s and temperatures of 20, 100, 200 and 300 °C. Friction coefficients were obtained by the software attached to HT−500. Wear loss was measured by a TG328B analytical balance with precision of 0.1 mg. Worn surface was analyzed by a FEIQUANTA200 scanning

electron microscope (SEM) with energy dispersive X-ray (EDX) spectrometer. Microhardness was tested by a DHV−1000 microhardness tester at 4.9 N for a dwelling time of 15 s.

3 Results and discussion

3.1 Effects of loads on tribological properties of TiC$_P$/Ni-based alloy composite coatings

The friction and wear results of the TiC$_P$/Ni-based alloy composite coatings at different loads are shown in Fig. 1. It shows that the friction coefficients and wear losses of the composite coatings are smaller than those of the Ni-based alloy coatings. With the loads rising from 3 to 12 N, the friction coefficients (μ) of the composite coatings take on an ascending trend from 0.343 to 0.402, which of the Ni-based alloy coatings change in a higher range of 0.359−0.419 (Fig. 1(a)). The wear losses (M) of the composite coatings rise from 2.2 to 6.2 mg as the loads increase, but are decreased by 14.6%−29.1% compared with those of the Ni-based alloy coatings (Fig. 1(b)).
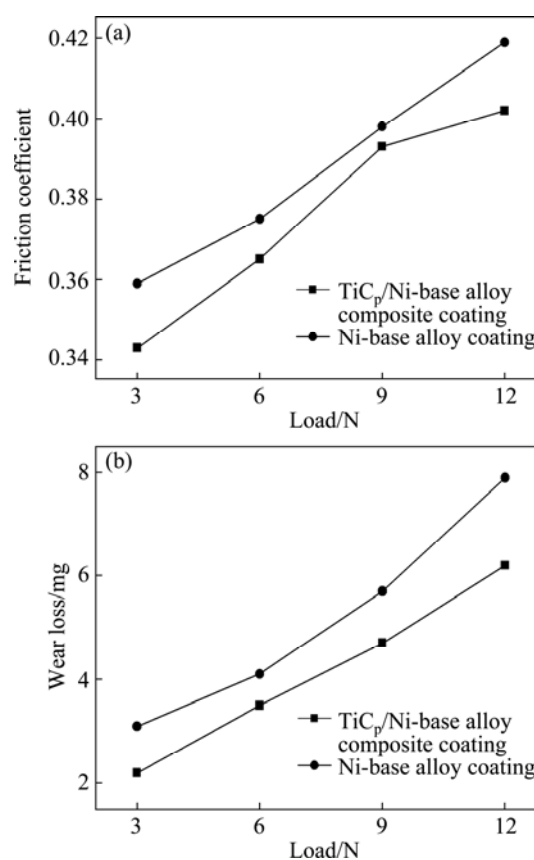

Fig. 1 Friction coefficients (a) and wear losses (b) of TiC$_P$/Ni-base alloy composite coatings at different loads

Since the microhardness of the composite coatings reaches HV$_{0.5}$686.7, and is 12.6% higher than that of the Ni-base alloy coatings, so the composite coatings have

stronger plastic deformation resistance. Meanwhile, the uniformly distributed TiC particles acting as pinning effect can change the dislocation direction and block the yield flow of the Ni-base alloy matrix to alleviate friction-induced plastic deformation. Besides, as the load-bearing phase, TiC particles can reduce the contact stress on the Ni-base alloy matrix and decrease the contact area between friction surfaces to relieve the abrasion caused by the GCr15 steel ball. Therefore, the TiC$_P$/Ni-base alloy composite coatings exhibit better antifriction and antiwear properties than the Ni-base alloy coatings.

Figure 2 presents the worn surface morphologies of the composite coatings at different loads. At the light load of 3 N, there are a few scratches appearing on the worn surface (Fig. 2(a)). The composite coating is in slight wear condition and experiences micro-cutting wear due to the abrasion among asperities of the friction surfaces. However, the worn surface becomes rough at the heavy load of 12 N, that is, obvious plastic deformation and delamination accompanied with plenty of cracks and fractured desquamation are observed in Fig. 2(b). In particular, the worn surface shows high microhardness of HV$_{0.5}$712.4 compared with the unworn surface indicating obvious work hardening. As the loads increase, the composite coatings bear higher contact stress and result in severe plastic deformation. After
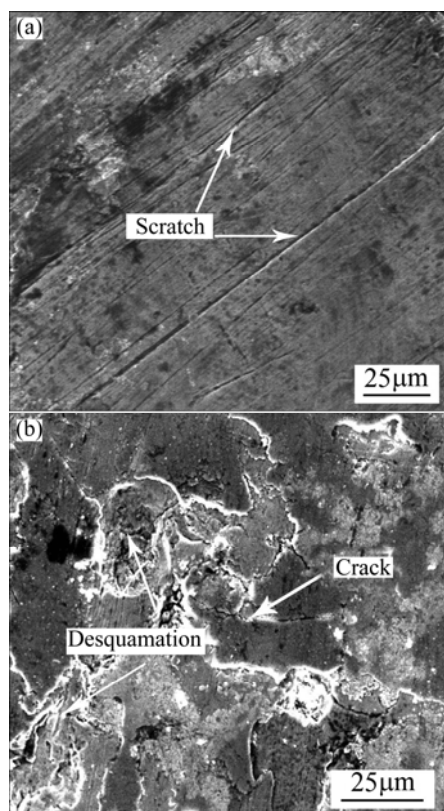
repeating ploughing and extruding by the GCr15 steel ball, the worn surface suffers from work hardening and its brittleness increases [18]. Cracks are prone to initiate and extend in friction process, and finally lead to brittle fracture of the worn surface. Evidently, the composite coatings are dominated by multi-plastic deformation wear and micro-brittle fracture wear at 12 N.
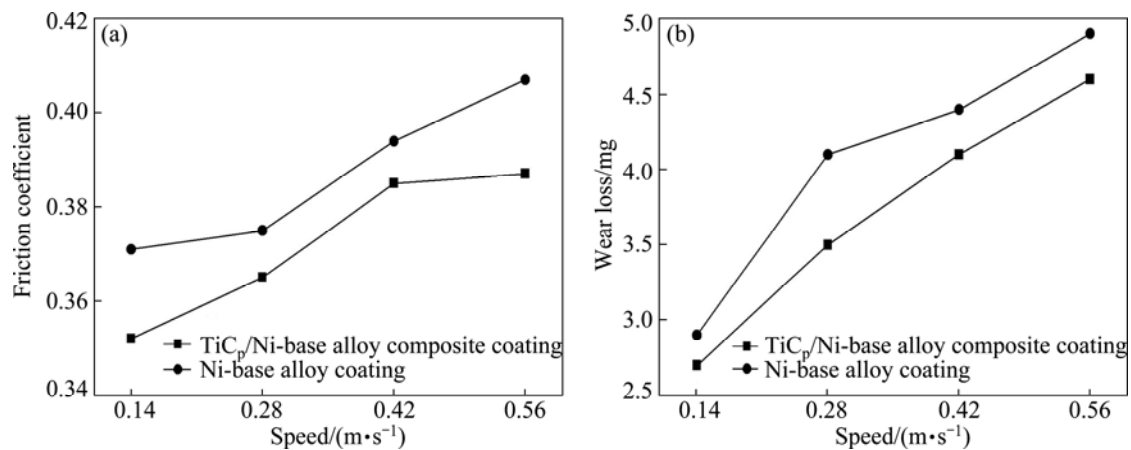
3.2 Effects of speeds on tribological properties of TiC$_P$/Ni-base alloy composite coatings

The friction coefficients and wear losses of the TiC$_P$/Ni-base alloy composite coatings at different speeds are shown in Fig. 3. It is obvious that the composite coatings own smaller friction coefficients than the Ni-base alloy coatings. When the speeds (V) are lower than 0.42 m/s, the friction coefficients of the composite coatings increase from 0.352 to 0.385, and keep a steady variation in the range of 0.385−0.387 at the speeds higher than 0.42 m/s (Fig. 3(a)). As the speeds increase from 0.14 to 0.56 m/s, the wear losses of the composite coatings also rise from 2.7 mg to 4.6 mg. The average value is 8.6% less than that of the Ni-base alloy coating (Fig. 3(b)).

Figure 4 depicts the worn surfaces morphologies and EDX spectra of the composite coatings at typical speeds. It is found that at the low speed of 0.14 m/s, the worn surface is flat but with some slight scratches and small wear debris probably caused by the mutual abrasion between the surface asperities (Fig. 4(a)). The worn surface contains Ni, Cr, Si and Fe according to the EDX spectrum of area A, indicating that it is the Ni-base alloy matrix (Fig. 4(c)). At the speed of 0.42 m/s, the worn surface shows plastic deformation, cracks and fatigue fractured desquamation. The EDX spectrum of area B on the worn surface shows a higher content of element O than that at 0.14 m/s (Figs. 4(b) and (d)). It can be inferred that the metal oxide films formed on the worn surface function as antifriction [19], so the friction coefficients hardly change when the speeds are higher than 0.42 m/s. As the speeds increase, plenty of frictional heat is generated on the contact areas. The strength and hardness of surface materials are declined due to heat softening. Therefore, the composite coatings suffer from multi-plastic deformation wear by repeating abrasion and plough. Besides, high speeds increase the contact frequency between friction surfaces, which may accelerate the cracks initiation and propagation during the friction process and result in fatigue fracture wear.

3.3 Effects of temperatures on tribological properties of TiC$_P$/Ni-base alloy composite coatings

The variation of friction coefficients and wear losses of the TiC$_P$/Ni-base alloy composite coatings with temperatures (t) is depicted in Fig. 5. It can be seen that

Fig. 2 SEM images of worn surfaces of TiC$_P$/Ni-base alloy composite coatings at 3 N (a) and 12 N (b)

Fig. 3 Friction coefficients (a) and wear losses (b) of TiC_P/Ni-base alloy composite coatings at different speeds
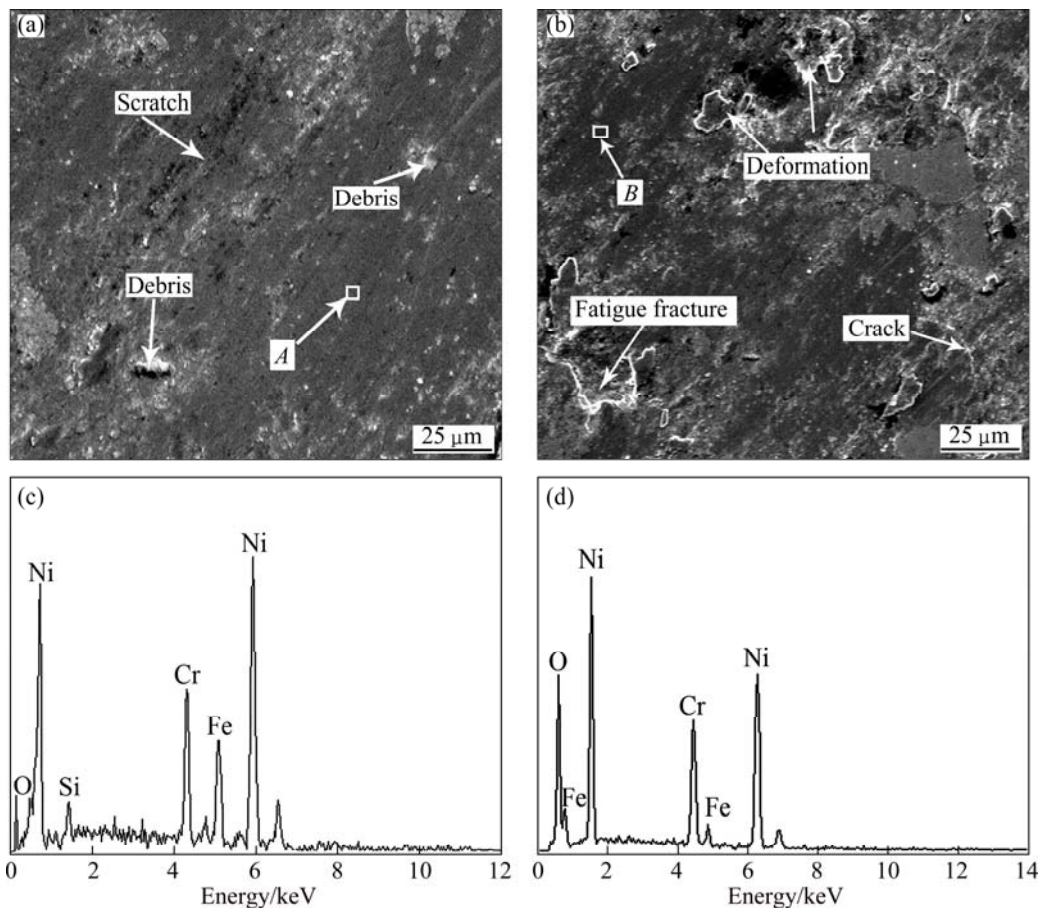
Fig. 4 SEM images of worn surfaces of TiC_P/Ni-base alloy composite coatings at 0.14 m/s (a) and 0.42 m/s (b), and EDX spectra of area A (c) and area B (d)

the friction coefficients of the composite coatings vary in the range of 0.365−0.410, which are slightly smaller than those of the Ni-base alloy coatings in the range of 0.375−0.432 (Fig. 5(a)). The wear loss of the composite coatings at 20 °C is 3.5 mg, which sharply increases to 5.6 mg at 300 °C, but is still 23.3% less than that of the Ni-base alloy coatings (Fig. 5(b)).

Figure 6 illustrates the worn surface morphology of

the composite coatings at 300 °C. It shows that severe plastic deformation and adhesive desquamation as well as plenty of wear debris are formed on the worn surface. Because of the increasing temperature, the mechanical behavior and plastic deformation resistance of the composite coatings are reduced, so the multi-plastic deformation wear occurs during the friction process. Additionally, the elevated temperature improves element
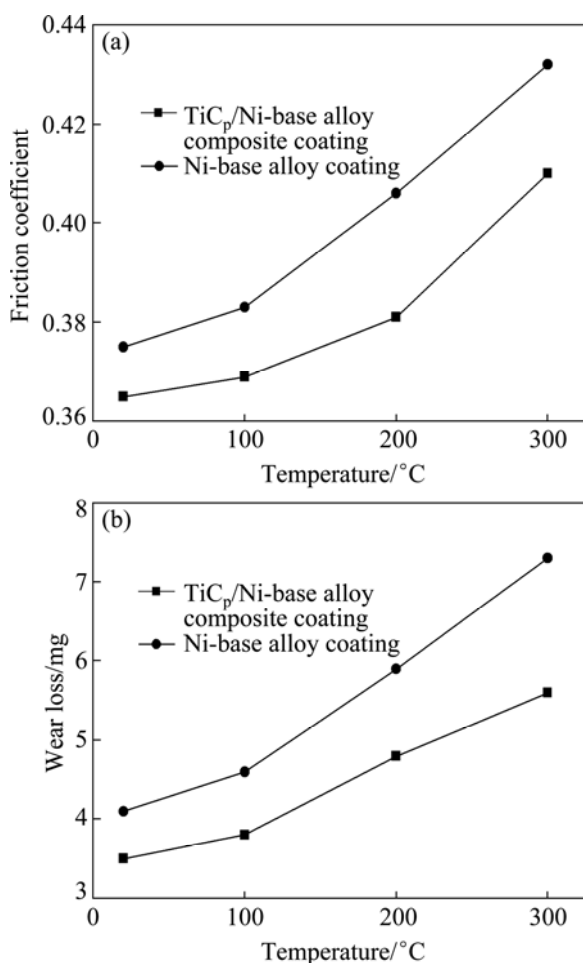
Fig. 5 Friction coefficients (a) and wear losses (b) of TiC_P/Ni-base alloy composite coatings at different temperatures
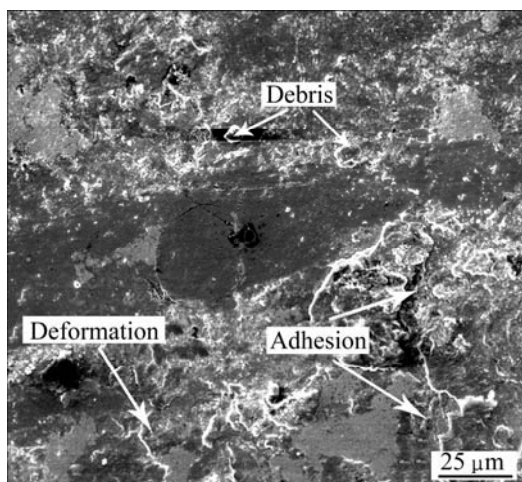

Fig. 6 SEM image of worn surface of TiC_P/Ni-base alloy composite coatings at 300 °C

diffusion between the composite coating and the GCr15 steel ball, which leads to cold welding in the contact area [20]. Under the action of tangential friction, the worn surface is avulsed, so the friction coefficients and wear losses of the composite coatings are sharply increased.

4 LS-SVM wear prediction model

4.1 Foundation of prediction model

The tribological behavior and mechanisms of the composite coatings rest with many factors. In the friction process, load, speed and temperature can notably change the stress field and temperature field on the friction surfaces, furthermore, influence the tribological behavior of the composite coatings. Besides, the actual working actions of friction parts are achieved by the variation of load, speed and temperature. Moreover, the three factors are easy to fulfill quantitative control and experimental validation. Consequently, load, speed and temperature are selected as input variables, and friction coefficient and wear loss are used as output variables in this work to carry out the tribological behavior prediction of the TiC_P/Ni-base alloy composite coatings under multiple factors by LS-SVM. Actually, the variables are the experimental results, so the influence conditions of lubrication, humidity and contact model on tribological properties have been considered.

Supposing that the data vector set in the given experimental conditions is $\theta=\{x_i, y_i\}$, $i=1, 2, \cdots, N$, that the input variables vector set is $x_i=\{x_{1i}, x_{2i}, x_{3i}\}=\{$load, speed, temperature$\}$, $x_i \in R^3$, and the output variables vector set is $y_i=\{y_{1i}, y_{2i}\}=\{$friction coefficient, wear loss$\}$, $y_i \in R^2$.

Define a nonlinear mapping of $\varphi(x)$ to transform vector sets from nonlinear space to high-dimension linear space based on the principle of LS-SVM, the linear relationship between the input and output variables can be found as follows:

$$y(x) = \boldsymbol{\omega}^{\mathrm{T}}\boldsymbol{\varphi}(x) + b \tag{1}$$

where $\boldsymbol{\omega}$ is the weight vector, and b is the bias term.

Take random errors into consideration, the prediction of tribological behavior can be ascribed to solve the following optimized target function [21]:

$$\min Q(\boldsymbol{\omega}, e_i) = \frac{1}{2}\boldsymbol{\omega}^{\mathrm{T}}\boldsymbol{\omega} + \frac{\gamma}{2}\sum_{i=1}^{N} e_i^2 \tag{2}$$

Subject to equality constraints

$$y_i = \boldsymbol{\omega}^{\mathrm{T}}\boldsymbol{\varphi}(x_i) + b + e_i, i = 1, 2, \cdots, N \tag{3}$$

where γ is the penalty factor, e_i is the random errors.

To solve this optimization problem, a Lagrange function is constructed as follows:

$$L(\boldsymbol{\omega}, b, e, \alpha) = \frac{1}{2}\boldsymbol{\omega}^{\mathrm{T}}\boldsymbol{\omega} + \frac{\gamma}{2}\sum_{i=1}^{N} e_i^2 - \sum_{i=1}^{N}\alpha_i(\boldsymbol{\omega}^{\mathrm{T}}\boldsymbol{\varphi}(x_i) + b + e_i - y_i) \tag{4}$$

where α_i is the Lagrange multiplier.

And then, the partial derivative of Eq. (4) is obtained and set zero to create the following equations:

$$\begin{cases} \dfrac{\partial L}{\partial \omega} = 0 \Rightarrow \omega = \sum_{i=1}^{N} \alpha_i \phi(x_i) \\ \dfrac{\partial L}{\partial b} = 0 \Rightarrow \sum_{i=1}^{N} \alpha_i = 0 \\ \dfrac{\partial L}{\partial e_i} = 0 \Rightarrow \alpha_i = \gamma e_i \\ \dfrac{\partial L}{\partial \alpha_i} = 0 \Rightarrow \omega^{\mathrm{T}} \phi(x_i) + b + e_i - y_i = 0 \end{cases} \quad (5)$$

Eliminate parameters ω and b, the matrix formation of Eq. (5) is established, i.e.,

$$\begin{bmatrix} 0 & \boldsymbol{u}^{\mathrm{T}} \\ \boldsymbol{u} & \boldsymbol{\Omega} + \gamma^{-1} \boldsymbol{I}_N \end{bmatrix} \cdot \begin{bmatrix} b \\ \alpha \end{bmatrix} = \begin{bmatrix} 0 \\ y \end{bmatrix} \quad (6)$$

where $\boldsymbol{y}=[y_1, y_2, \cdots, y_N]^{\mathrm{T}}$, $\boldsymbol{u}=[1,1,\cdots,1]^{\mathrm{T}}$, $\boldsymbol{\alpha}=[\alpha_1, \alpha_2, \cdots, \alpha_N]^{\mathrm{T}}$, and $\boldsymbol{I}_N$ is the identity matrix of order N.

Therefore, the solution of Eq. (6) is as follows:

$$\begin{cases} b = \dfrac{\boldsymbol{u}^{\mathrm{T}}(\boldsymbol{\Omega} + \gamma^{-1} \boldsymbol{I}_N)^{-1} \boldsymbol{y}}{\boldsymbol{u}^{\mathrm{T}}(\boldsymbol{\Omega} + \gamma^{-1} \boldsymbol{I}_N)^{-1} \boldsymbol{u}} \\ \alpha = (\boldsymbol{\Omega} + \gamma^{-1} \boldsymbol{I}_N)^{-1}(\vec{\boldsymbol{y}} - \boldsymbol{u}b) \end{cases} \quad (7)$$

According to the Mercer law, the parameter Ω can be expressed by

$$\boldsymbol{\Omega} = \varphi(x_i)^{\mathrm{T}} \varphi(x_j) = K(x_i, x_j), i, j = 1, 2, \cdots, N \quad (8)$$

where $K(x_i, x_j)$ is the nonlinear kernel function.

The function, as long as fitting the Mercer law, can be used as the kernel function. For example, Gauss radial basis function (RBF) can simplify the calculated process and improve the generalization performance [22], which is selected as the kernel function in this model, i.e.,

$$K(x_i, x_j) = \exp\left\{-\left\|x_i - x_j\right\|^2 / \sigma^2\right\} \quad (9)$$

where σ is the kernel width.

As discussed above, the LS-SVM prediction model on tribological behavior of the composite coatings can be expressed as

$$y(x) = \sum_{i=1}^{N} a_i K(x, x_i) + b \quad (10)$$

where x_i is the input variables of load, speed and temperature, and $y(x)$ is the output variables of friction coefficient and wear loss.

4.2 Predictive results and comparison

For accurately predicting the tribological behavior of the TiC$_P$/Ni-base alloy composite coatings under dry friction conditions, 22 experiments were carried out at different loads, speeds and temperatures based on single-factor experiment. The experimental conditions are listed in Table 1. Training samples include the first 17 groups of data, and the rest 5 groups of data are used as the predictive samples.

Table 1 Testing conditions and wear results

No.	F/N	v/(m·s^{-1})	t/°C	μ	m/mg
1	3	0.28	20	0.343	2.2
2	9	0.28	20	0.393	4.6
3	12	0.28	20	0.402	6.2
4	6	0.14	20	0.352	2.7
5	6	0.28	20	0.365	3.5
6	3	0.42	200	0.368	3.5
7	6	0.56	20	0.387	4.6
8	6	0.28	100	0.369	3.8
9	6	0.28	200	0.381	4.8
10	9	0.14	100	0.397	4.7
11	12	0.14	200	0.438	6.7
12	12	0.56	200	0.426	7.1
13	12	0.14	100	0.418	6.1
14	9	0.56	300	0.447	6.9
15	3	0.56	300	0.389	5.1
16	9	0.42	300	0.43	6.3
17	3	0.42	100	0.377	2.8
18	6	0.42	20	0.385	4.1
19	6	0.28	300	0.41	5.6
20	12	0.42	300	0.446	7.3
21	9	0.56	200	0.413	5.8
22	3	0.14	100	0.351	2.7

Because the experimental data are different in dimension, the predictive accuracy of LS-SVM model may be affected. Therefore, prior to prediction, the input data are normalized using the following formula:

$$a^* = \frac{a - a_{\min}}{a_{\max} - a_{\min}} \quad (11)$$

where a is the input data, $a_{\max}$ and $a_{\min}$ are the maximum and minimum value of input data, respectively, and a^* is the normalized variables.

After prediction, anti-normalization of the output data is performed to obtain the actual values. Penalty factor γ and kernel width σ are 79 and 10 after several optimized processes. Root mean square error (RMSE) characterizes the deviation extent between the real values and predictive values, which is expressed as follows [23]:

$$\mathrm{RMSE} = \sqrt{\frac{1}{n} \sum_{i=1}^{n} \left(\frac{y_i - Y_i}{Y_i}\right)^2} \quad (12)$$

where *n* is the sample capacity, y_i is the predictive value, and Y_i is the real value.

The predictive results utilizing the LS-SVM model are listed in Table 2. Besides, a BP-ANN model is trained with the same data, and the comparison in predictive effects between the BP-ANN model and the LS-SVM model is listed in Table 3. Obviously, the predictive values of friction coefficients and wear losses by the LS-SVM model are close to the real values. The RMSEs of friction coefficients and wear losses are 3.14% and 5.11%, respectively, which are smaller than the BP-ANN model of 7.61% and 8.79%. In addition, the LS-SVM model shows much short predicting time of 0.121 s compared with the BP-ANN model. It can be concluded that the LS-SVM model takes on fast and accurate predicting ability. This is because that the BP-ANN model needs large training samples, its accurate prediction is hard to achieve with small samples. However, the LS-SVM model has better generalization performance, and enables to carry out the accurate prediction using small samples.

Table 2 Predictive results by LS-SVM model

No.	Friction coefficient			Wear loss		
	Real	Predictive	Error/%	Real/mg	Predictive/mg	Error/%
18	0.385	0.376	2.33	4.1	3.944	3.81
19	0.410	0.402	1.95	5.6	5.438	2.89
20	0.446	0.452	−1.35	7.3	6.929	5.08
21	0.413	0.403	2.42	5.8	6.066	−4.58
22	0.3510	0.371	−5.69	2.7	2.911	−7.81

Table 3 Comparison in predictive effects between LS-SVM model and BP-ANN model

Model	Calculating time/s	RMSE/%	
		Friction coefficient	Wear loss
LS-SVM	0.121	3.14	5.11
BP-ANN	0.936	7.61	8.79

5 Conclusions

1) The TiC_P/Ni-base alloy composite coatings show higher microhardness and lower friction coefficients and wear losses than the Ni-base alloy coatings. As the loads rise from 3 N to 12 N, the friction coefficients increase from 0.343 to 0.402, and the wear losses vary in the range of 2.2−6.2 mg. At the speeds lower than 0.42 m/s, the friction coefficients increase from 0.352 to 0.385, and keep steady at the speeds higher than 0.42 m/s. The wear losses change in the range of 2.7−4.6 mg at different speeds. At the temperatures of 20−300 °C, the friction coefficients and wear losses vary in the range of 0.365−0.41 and 3.5−5.6 mg, respectively.

2) The wear mechanism of the composite coatings is micro-cutting wear at the low load of 3 N or speed of 0.14 m/s. As the loads rise to 12 N, the wear mechanisms become multi-plastic deformation wear and micro-brittle fracture wear, which turn into multi-plastic deformation wear and fatigue wear at 0.42 m/s. At 300 °C, the composite coatings suffer from multi-plastic deformation wear and adhesive wear.

3) The predicting time of the LS-SVM model is 0.121 s, which is less than that of the BP-ANN model of 0.936 s. The RMSE of friction coefficients and wear losses by the LS-SVM model are 3.14% and 5.11%, which are reduced by 58.74% and 41.87% compared with the BP-ANN model. The LS-SVM model can fulfill the fast and accurate prediction on tribological behavior of the composite coatings under different friction conditions.

References

[1]   LOZANO D E, MERCADO-SOLIS R D, PEREZ A J, TALAMANTES J, MOLARES F, HERNANDEZ-RODRIGUEZ M A L. Tribological behavior of cast hypereutectic Al−Si−Cu alloy subjected to sliding wear [J]. Wear, 2009, 267: 545−549.

[2]   MURAKAMI T, KAJINO S, NAKANO S. High-temperature friction and wear properties of various sliding materials against aluminum alloy 5052 [J]. Tribology International, 2013, 60: 45−52.

[3]   ZHANG H T, CUI J Z. Production of super-high strength aluminum alloy billets by low frequency electromagnetic casting [J]. Transactions of Nonferrous Metals Society of China, 2010, 21(10): 2134−2139.

[4]   KIM S J, JANG S K, HAN M S, PARK J C, JEONG J Y, CHONG S O. Mechanical and electrochemical characteristics in sea water of 5052-O aluminum alloy for ship [J]. Transactions of Nonferrous Metals Society of China, 2013, 23(3): 636−641.

[5]   SHI G D, WANG Z, WANG Y S, WU Z J, LIANG J. Effect of heat treatment on microstructure and tensile strength of NiCoCrAl alloy sheet fabricated by EB-PVD [J]. Transactions of Nonferrous Metals Society of China, 2012, 22(10): 2395−2401.

[6]   CHALIAMPALIAS D, VOURLIAS G, PAYLIDOU E, SKOLIANOS S, CHRISSAFIS K, STERGIOUDIS G. Comparative examination of the microstructure and high temperature oxidation performance of NiCrBSi flame sprayed and pack cementation coatings [J]. Applied Surface Science, 2009, 255: 3605−3612.

[7]   SERRES N, HLAWKA F, COSTIL S, LANGLADE C, MACHI F. Microstructures of metallic Ni-base alloy coatings manufactured via hybrid plasma spray and in situ laser remelting process [J]. Journal of Thermal Spray Technology, 2010, 12: 49−56.

[8]   GOMEZ T, GARRIDO M A, FERNANDEZ J E, CADENAS M, RODRIGUEZ J. Influence of the deposition techniques on the mechanical properties and microstructure of NiCrBSi coatings [J]. Journal of Materials Processing Technology, 2008, 204: 304−312.

[9]   CAI B, TAN Y F, TU Y Q, WANG X L, TAN H. Tribological properties of Ni-base alloy composite coating modified by both graphite and TiC particles [J]. Transactions of Nonferrous Metals Society of China, 2011, 21(11): 2426−2432.

[10] CAI B, TAN Y F, HE L, TAN H, GAO L. Tribological properties of TiC particles reinforced Ni-based alloy composite coatings [J]. Transactions of Nonferrous Metals Society of China, 2013, 23(6):

1681−1688.

[11] WANG D C, WANG M H, QIAO X J. Support vector machines regression and modeling of greenhouse environment [J]. Computers and Electronics in Agriculture, 2009, 66: 46−52.

[12] JIANG Shao-hua, GUI Wei-hua, YANG Chun-hua, DAI Xian-jiang. Fault diagnosis method based on rough set and least squares support vector machine and its application [J]. Journal of Central South University: Science and Technology, 2009, 40(2): 447−451. (in Chinese)

[13] SHU Fu-hua. Prediction model for extrusion force of Cu−0.75Cr alloy based on least square support vector machine [J]. The Chinese Journal of Nonferrous Metal, 2008, 18(9): 1706−1710. (in Chinese)

[14] GENCOGLU M T, UYAR M. Prediction of flashover voltage of insulators using least squares support vector machines [J]. Expert Systems with Applications, 2009, 36(7): 10789−10798.

[15] LU De-feng, ZUO Hong-fu, CAI Jing, WANG Ye. Research on an optimal algorithm for the prediction of wear loss [J]. Tribology, 2008, 28(6): 562−566. (in Chinese)

[16] WAN Yi. Method for analyzing the wearing characteristics of centrifugal pump based on support vector machines [J]. Journal of Hydraulic Engineering, 2010, 41(4): 488−452. (in Chinese)

[17] SHI D F, GINDY N N. Tool wear predictive model based on least squares support vector machines [J]. Mechanical Systems and Signal Processing, 2007, 21(4): 1799−1814.

[18] MENG Fan-jun, ZHU Sheng, BA De-ma. Microstructure and tribological performance of 45CrNiMoVA steel welded surface layer [J]. Chinese Journal of Mechanical Engineering, 2008, 44(4): 150−153. (in Chinese)

[19] ZHANG Xiao-yu, REN Ping-di, ZHANG Ya-fei, ZHU Min-hao, ZHOU Zhong-rong. Fretting wear behavior of Incoloy800 alloy at high temperature [J]. The Chinese Journal of Nonferrous Metals, 2010, 20(8): 1545−1551. (in Chinese)

[20] LIU H J, FENG X L. Microstructure and interfacial quality of diffusion bonded TC21 titanium alloy joints [J]. Transactions of Nonferrous Metals Society of China, 2011, 21: 58−64.

[21] ZHANG Y, LIU Y C. Data imputation using least squares support vector machines in urban arterial streets [J]. IEEE Signal Processing Letters, 2009, 16(5): 414−417.

[22] SONG Jiang-teng, ZENG Pan, ZHAO Jia-qing, LI Cong-cong. Analysis of stellite alloys wearing prediction based on radial basis function neutral network [J]. Lubrication Engineering, 2011, 36(3): 30−33. (in Chinese)

[23] HAN X W, SHAO M A, HORTON R. Estimating van Genuchten model parameters of undisturbed soils using an integral method [J]. Pedosphere, 2010, 20(1): 55−62.

TiC 颗粒增强镍基合金复合涂层的摩擦学性能及磨损预测模型

谭业发，何 龙，王小龙，洪 翔，王伟刚

解放军理工大学 野战工程学院，南京 210007

摘 要：运用等离子喷涂技术在铝合金表面制备 TiC$_p$/镍基合金复合涂层，研究干摩擦条件下载荷、速度和温度对复合涂层摩擦磨损行为与机理的影响规律；建立了基于最小二乘支持向量机(LS−SVM)的复合涂层磨损预测模型。结果表明：在不同摩擦条件下，TiC$_p$/镍基合金复合涂层的摩擦因数和磨损质量均低于镍基合金涂层。LS−SVM 模型对摩擦因数和磨损失重的预测时间仅为 BP−ANN 模型的 12.93%，其预测精度分别比 BP−ANN 模型提高了 58.74%和 41.87%，可有效预测干摩擦条件下 TiC$_p$/镍基合金复合涂层的摩擦磨损行为。

关键词：TiC 颗粒；镍基合金；复合涂层；最小二乘支持向量机(LS−SVM)；磨损预测模型

(Edited by Xiang-qun LI)